RSC Advances

ROYAL SOCIETY OF CHEMISTRY

www.rsc.org/advances

Synthesis gas production from bio-oil: steam reforming of ethanol as a model compound

S. Pavlova[1], P. Yaseneva[2], V. Sadykov[1], V. Rogov[1], S. Tikhov[1], Yu. Bespalko[1], S. Belochapkine[2], J. Ross[3]

[1]Boreskov Institute of Catalysis, Pr.Lavrentieva, 5, 630090, Novosibirsk, Russia;
[2]University of Cambridge, United Kingdom
[3]Materials & Surface Science Institute, Limerick, Ireland;
[4]University of Limerick, Limerick, Ireland

Using original hydrothermal technology honeycomb corundum monoliths with a peculiar porous structure and high water-adsorbing capacity facilitating procedures of active component loading have been produced. The detail study of ethanol steam reforming over Ru/$Ce_{0.5}Zr_{0.5}O_2$(CZ), Ru/$Ce_{0.4}Zr_{0.4}Sm_{0.2}O_2$-(δ+γ)$Al_2O_3$ (granulated) and Ru/$Ce_{0.4}Zr_{0.4}Sm_{0.2}O_2$/α-$Al_2O_3$(monolithic) has been performed. It has been revealed that the main route of the reaction over Ru/CZ is ethanol dehydrogenation while ethanol dehydration into ethylene is mainly occurs over Ru/CZS-Al_2O_3. Variation of the H_2O/EtOH ratio, contact time and temperature allows hydrogen and CO yield to be governed. The monolithic catalyst has shown a high performance and stability at short contact time (0.1-0.4 s) and low water concentration (H_2O/EtOH~1-3).

Key words: Ethanol steam reforming, syngas, Ce-Zr mixed oxides, Ru, honeycomb corundum monolith

1. Introduction

Nowadays, the major sources for energy and chemicals production are fossil fuels: crude, natural gas or coal. Biomass being renewable feedstock is an attractive alternative source with the advantages of its availability throughout the world and reduction of greenhouse emissions [1-2]. Fast pyrolysis of biomass is now a mature technology producing bio-oils (biodisel) which can be converted by its catalytic treatment to hydrogen or synthesis gas [3-5]. Bio-hydrogen and bio-syngas could be feedstocks for liquid fuels (gasoline, diesel) and valuable chemicals production and they are cleanest fuels for the different types of fuel cells, gas turbine, internal combustion engine as well [6-8]. Hence, this technology to produce syngas or hydrogen can be the most promising process for a clean and renewable fuel generation.

The most promising processes of bio-oil catalytic transformation into synthesis gas are known to be the steam and combined oxidative reforming. However, rapid deactivation of

current catalysts in these processes is a significant technological barrier, and design of highly stable, selective and active catalysts for novel, highly oxygenated feedstocks is a key option in solving this problem [6-12].

Since bio-oils are complex mixtures of oxygenated hydrocarbons including aliphatic and aromatic acids, aldehydes, ketones, alcohols, esters, the catalytic studies are usually carried out for typical examples of an individual compound class such as ethanol, acetic acid, acetone, glycerol et. [11-15]. A wide range of supported active metals (Ni, Co, Cu [13-14, 16-23], Pt, Pd, Rh, Ru [15, 24-28]) were used for the bio-oil reforming processes. However, they are subjected to strong coking being supported on traditional inert oxides [14-18, 24], while a high stability to coking and catalytic activity of metals is achieved when their nanoparticles are stabilized in the matrix of ceria-zirconia fluorite-like mixed oxides with high oxygen mobility that is due to participation of support oxygen in gasification of coke precursors [21-23, 25-28]. Incorporation of low-valence cations (such as La, Gd, Pr) into the lattice of ceria-zirconia solid solution improves the lattice oxygen mobility [29-30] that could increase coking stability of catalysts.

The catalysts are usually studied in reforming reactions as pellets obtained from corresponding powders which are unsuitable for practical applications because of pressure drop. Compared with them, catalysts loaded on structured supports have advantages such as lower pressure drop and larger external surface area per unit volume. However, there are only several works in which conversion of bio-oil or its components into synthesis gas or hydrogen has been studied over monolithic catalysts [31-36]. Thus, Ni/La_2O_3 and $Ru/\gamma\text{-}Al_2O_3$ supported on cordierite honeycomb and alumina-zirconia foam monoliths have shown good catalytic performance in partial oxidation of ethanol [31-32]. $Pt(Rh)/Ce_{0.5}Zr_{0.5}O_2$ supported on cordierite monolith [35] and $Rh\text{-}CeO_2/\gamma\text{-}Al_2O_3$ loaded on $\alpha\text{-}Al_2O_3$ foam monolith have been tested in steam reforming of real bio-oil [36].

In previous work using combinatorial approach [37], we studied in ethanol steam reforming (ESR) a large number of catalysts based on Al_2O_3 loaded with Ce-Zr mixed oxides doped by La, Sm, Pr and different active metals (Cu, Cu-Ni, Ru, Pt, etc.). The results revealed that the most effective catalyst composition is $Ru/Ce_{0.4}Zr_{0.4}Sm_{0.2}\text{-}Al_2O_3$. Herein, we report the detail study of ESR for production of synthesis gas over Ru supported on ceria-zirconia and $Ce_{0.4}Zr_{0.4}Sm_{0.2}\text{-}Al_2O_3$. The catalyst $Ru/Ce_{0.4}Zr_{0.4}Sm_{0.2}$ was also tested being supported on a corundum monolith. The influence of a support nature and such ESR process parameters as feed composition, contact time and temperature is studied to achieve a high yield of syngas with a given composition.

2. Experimental

2.1. Catalysts

As supports, $Ce_{0.5}Zr_{0.5}O_2$(CZ) and 10%$Ce_{0.4}Zr_{0.4}Sm_{0.2}$-Al_2O_3 (CZS-Al_2O_3) were used. CZ was prepared by modified sol-gel method [38]. An aqueous solution of $Ce(NO_3)_3 \cdot 6H_2O$ (20 ml) was added to the zirconium butoxide $Zr(OC_4H_9)_4$ dissolved in 20 ml of butanol. A pseudogel formed was dried and calcined in air at 900°C for 2 h.

To prepare CZS- Al_2O_3, γ-Al_2O_3 (CONDEA Puralox SBa – 150, 150 m^2/g) stabilized by 5%wt. of La was impregnated with mixed solution of Ce, Sm nitrates and $ZrO(NO_3)_2$, dried overnight in air at 85°C and then calcined at 800°C [37].

The catalysts 1.4% Ru/$Ce_{0.5}Zr_{0.5}$(Ru/CZ) and 1.4%Ru/10%$Ce_{0.4}Zr_{0.4}Sm_{0.2}$-Al_2O_3(Ru/CZS-Al_2O_3) were synthesized by the standard wet impregnation of supports with a water solution of $RuOHCl_3$ followed by drying and calcination at 800°C in air. Main characteristics of these catalysts were reported elsewhere [37].

The specific surface area (BET area) was determined by the express BET method using Ar thermodesorption data obtained on a SORBI-M instrument. The XRD patterns were recorded using a URD-6M diffractometer with Cu K_α radiation in the range of 2θ angles 10–90°.

Honeycomb corundum monoliths of 50 mm diameter and 25 mm length with a peculiar porous structure (Fig. 1) were obtained using original hydrothermal technology (HTT) [39]. The aluminum powder (a commerical PA-4 grade) and aluminum hydroxide were used as raw materials. To form the transport microchannels along the monolith, easily burned organic fibers were inserted into the matrix before hydrothermal treatment stage (HTT) by a proprietary procedure. The mixture of aluminium and its hydroxide loaded into the special die was subjected to HTT at 100°C followed by calcination in air at 1200°C. During these procedures the total oxidation of metal aluminum occurs. The total pore volume of the monolith was estimated from the values of true and apparent densities. Its true density was measured using a helium pycnometer – Autopycnometer 1320 (Micromeritics). The share of micropores and mesopores as well as a specific surface area were determined from adsorption isotherms of nitrogen recorded at 77 K using the ASAP-2400 Micromeritics instrument.

The monolithic catalyst containing 1%Ru - 8%$Ce_{0.4}Zr_{0.4}Sm_{0.2}O_2$ was prepared by subsequent loading of the mixed oxide and Ru using impregnation of the support with corresponding water solutions followed by drying and calcination at 800°C.

2.2. Catalystic tests

ESR over catalysts pellets were carried out in U-shaped tubular quartz plug-flow reactor (4.5 mm i.d.) at atmospheric pressure. Usually 0.18 g of pelletized catalyst (fraction 0.5-0.25 mm) diluted in a 1:10 weight ratio with quartz sand was taken. Reaction was performed at 300-

800°C and 3300-50000 h^{-1} GHSV (0.07-1s contact time) using the gas feed containing 10 vol.% C_2H_5OH, 15-50 vol. % H_2O (the corresponding molar ratio H_2O:C_2H_5OH = 1.5 ÷ 5), N_2 balance. Before testing the catalysts were pre-treated for 1 hour at 400 °C in the flow of 10 % H_2 in N_2. Three on-line gas chromatographs (GC) "LHM-8" equipped with thermal conductivity detectors and a flame ionization detector were used for the analysis of reactants and products. Hydrocarbons (CH_4, C_2H_6, C_2H_4, etc.) and oxygenates (EtOH, CH_3OH, acetone, diethyl ether, etc) were analyzed using a Porapak T column; N_2, O_2, CH_4 and CO were analyzed with a molecular sieve column, and H_2, N_2, CO, CO_2, CH_4 – with an active carbon "SYT" column. Ar and He were used as carrier gases.

Ethanol conversion (X_{EtOH}), selectivity to carbon products (S_i) and hydrogen yield (Y_{H2}) were calculated according to the next equations:

$$x_{EtOH} = \frac{mol_{EtOH}^{in} - mol_{EtOH}^{out}}{mol_{EtOH}^{in}} \times 100\% ,$$

$$S_i = \frac{\nu_i \cdot mol_i}{\sum_i^n \nu_i \cdot mol_i} \times 100\% ,$$

$$Y_{H_2} = \frac{mol_{H_2}}{6 \cdot mol_{EtOH}^{in}} \times 100\% ,$$

where ν_i is the number of carbon atoms in "*i*" product.

The monolithic catalyst was tested in a pilot reactor in the gas feed with C_2H_5OH concentration of 13 vol. %, H_2O concentration of 14-60 vol.% corresponding to H_2O:C_2H_5OH molar ratio of ~ 1.1-4.7 at 700-750°C and contact time of 0.03-0.1 s. The temperature of the monolithic catalyst has been measured at its exit. The analysis of the main reaction products (H_2, CO, CO_2, CH_4) was carried out with on-line GC.

3. Results and discussion

3.1. Characterization of catalysts

The BET surface area of CZ calcined at 900°C was 9 m^2/g while in the case of Ru/CZS-Al_2O_3 it is equal 110 m^2/g. Thus, successive deposition of CZS and Ru on γ-Al_2O_3 having the initial surface area 150 m^2/g led to a moderate decrease of the surface area.

The BET surface of the corundum monolith was ~ 2.6 m^2/g. The total pore volume was close to 0.4 cm^3/g. The absence of hysteresis on the nitrogen adsorption isotherm evidences that micropores are missing. The volume of mesopores is substantially small (~ 0.005 cm^3/g). Thus, the pore structure of corundum monoliths is namely formed by macropores and ultramacropores with a size of 1μm and more that provides a high diffusion permeability of the monolith walls.

Ultramacropores of the size in the range from 1 to 10 μm with the average value of 1-2 μm are clearly visible in SEM images of the monolith cross-section (Fig. 2 b, c). The surface of channel walls is highly rough (Fig. 2 a): a height difference reaches tens of μm. Thus, these peculiarities of porous structure gives sufficiently high water-absorbing capacity, keeps a high dispersion of supported active component and provides a higher thermal shock stability of cermet monoliths as compared with honeycombs prepared by extrusion (Fig.1). A high water absorption capacity simplifies procedures of the active component loading on the monolith support: a common method of incipient wetness impregnation was used instead of washcoating requiring repeated supporting of the catalyst suspension on the substrate.

According to XRD data, $Ce_{0.5}Zr_{0.5}O_2$ is a mixture of $Ce_{0.76}Zr_{0.24}O_2$ and $Ce_{0.45}Zr_{0.55}O_2$ cubic solid solutions with lattice parameters 5.354 and 5.248 Å, respectively. Raman spectroscopy being a very sensitive to the structure shows that a metastable tetragonal phase t'' is present along with a cubic phase. Indeed, in the Raman spectrum, the main band at 472 cm^{-1} corresponding to a cubic solid solution is asymmetrical with a shoulder at 535 cm^{-1} and, additionally, a low intensity band at 310 cm^{-1} is observed (Fig. 3). As shown earlier [37], for CZS-Al_2O_3, the main phases are fluorite-like cubic solid solution (JCPDS 43-1002) and mixed δ- and γ-Al_2O_3. The monoliths are mainly comprised of α-Al_2O_3 with a small admixture of δ-Al_2O_3. For both Ru-containing catalysts, the reflections of RuO_2 phase (JCPDS 71-2273) are observed.

3.2. Steam reforming of ethanol

3.2.1. Blank experiments

The data of the blank experiment without a catalyst allow evaluation of the thermal decomposition of ethanol. Its thermal conversion is low at temperatures below 750°C and substantially increases only at and above 750°C (Fig. 4). The yield of H_2 in the blank experiment is low in the whole temperature range with main products being CO, CH_4, acetaldehyde, C_2H_4 and C_2H_6 (Fig. 4, 5). A sufficiently high selectivity to CO and CH_4 at all temperatures evidences ethanol cracking while a high selectivity to acetaldehyde at temperatures below 750°C and to C_2H_4 at temperatures above 750°C shows realization of the gas-phase dehydrogenation and dehydration, respectively, catalyzed by quartz reactor walls.

3.2.2. Influence of support nature.

The influence of a support nature on ESR parameters has been studied in the feed with H_2O:EtOH molar ratio being equal 1:4 at the contact time of 0.07 s. Temperature dependence of

ethanol conversion, hydrogen yield and product selectivity over CZS-Al_2O_3, Ru/CZS-Al_2O_3, Ru/CZ is presented in Figs. 4, 6. Over all catalysts, the conversion of ethanol changes with temperature depending on the catalyst support. For Ru/CZ, ethanol conversion continuously increases from 37% up to 100% at temperature rising from 650 to 825°C. In the case of Ru/CZS-Al_2O_3, the conversion being equal 100% at 650 °C passes through the minimum at 700-750°C and reaches again the value of 100% at 800°C. Such a behavior is conditioned by the participation of a support in ESR. Indeed, the similar temperature dependence of the ethanol conversion is observed for CZS-Al_2O_3 with a pronounced drop at 700°C and continuously increasing up to 90% at 825°C.

It is known that ethanol conversion over Al_2O_3 could be close to 100% already at 350°C with C_2H_4 as a main product of ethanol dehydration on acid centers [40-41]. Ethanol adsorbs on the surface of Al_2O_3 with formation of ethoxy species which are transformed into highly stable acetate species at increasing temperature up to 700°C thus sharply decreasing ethanol conversion. At further temperature rising, acetate species are decomposed and the ethanol conversion increases. It may be stated that the same processes occur over CZS-Al_2O_3. For Ru/CZS-Al_2O_3, acetate species hinder the migration of ethoxide species toward Ru particles where they are decomposed. As a result, only the minor decrease of ethanol conversion is observed due to facile decomposition of ethoxide and acetate species on the metal-support boundary [26, 41-42].

The high C_2H_4 selectivity over CZS-Al_2O_3 and Ru/CZS-Al_2O_3 at 650-700 °C evidences preferential realization of ethanol dehydration, while for Ru/CZ the high selectivity to acetaldehyde and methane (at 650° ~30 and ~20%, correspondingly) is a result of ethanol dehydrogenation followed by decarbonylation of acetaldehyde [11]. The temperature dependence of selectivity to acetaldehyde is different for Ru/CZ and Ru/CZS-Al_2O_3 (CZS-Al_2O_3): it decreases gradually when temperature increases and passes through the maximum, correspondingly. Dependences similar to the case of Ru/CZ are usually observed for the catalysts where reaction mechanism includes ethanol dehydrogenation with formation of acetaldehyde and its decomposition at high temperature [11, 26]. The extremal temperature dependence of selectivity to acetaldehyde for Ru/CZS-Al_2O_3 (CZS-Al_2O_3) is determined by the parameters of catalyst testing in ESR as demonstrated in our experiments with a higher H_2O/EtOH raio and a longer contact time (see below).

Hydrogen yield over CZS-Al_2O_3 is low. Ru-containing catalysts show practically the same high values independent on the support type while selectivity to C-products is strongly influenced by the support nature (Table 1, Fig. 4, 6). Thus, H_2/CO values and CO_2 selectivity are higher for Ru/CZ in the whole temperature range. Note that in the case of CZS-Al_2O_3, CO_2 is absent in the

reaction products. The same effect was observed for $CeZrO_2$ in [22]. Using DRIFTS, the authors had shown that at high temperature, over $CeZrO_2$, in contrast to the results observed for $Pt/CeZrO_2$, significant amounts of acetate species were detected at the surface and there was no CO_2 formation over $CeZrO_2$ alone. Thus, the presence of Ru active metal promotes acetate decomposition and carbonate formation at high temperature, which could occur at the metal–support interface.

Selectivity to methane, in the case of CZS-Al_2O_3 support, being low at 650 °C gradually increases with temperature rising up to 825 °C as a result of thermal decomposition of ethanol which is in agreement with a low selectivity to target products (H_2, CO, CO_2) (Fig. 6). Over Ru/CZS-Al_2O_3, it passes through the maximum at 750°C due to methane conversion via steam reforming at high temperature. For Ru/CZ, at 700-825°C methane selectivity is close to one over Ru/CZS-Al_2O_3 while at 650°C its value is much higher due to decarbonylation of acetaldehyde [6, 11].

3.2.3. Effect of contact time and water/EtOH ratio

Temperature dependence of ethanol conversion, hydrogen yield and products selectivity in the low temperature region (350-700°C) at contact times of 0.46 and 1 s is presented in Figs. 7-8. The data show that though ethanol conversion is already high (80-100 %) at 400°C and slightly dependent on contact time, the yield of hydrogen strongly changes with the contact time. At contact time of 0.46 s, the yield is low in the temperature range of 350-600°C and reaches ~28% only at 700 °C, while its value is equal to ~30% at 500°C and increases up to 60% at 700°C for the contact time of 1 s (Fig. 8). The temperature dependence of the selectivity to C-products shows that at the short contact time, the main product is ethylene up to 700°C. For contact time of 1 s, selectivity to ethylene passes through the maximum (~90%) at 400 °C and decreases to zero at 600°C. Selectivity to CO gradually increases with the temperature rise while selectivity to CO_2 and methane reaching maximum at 600°C decreases at further temperature rising that is due to occurring RWGS and steam reforming of methane, respectively, which are facilitated at long contact times and high temperature [6, 11].

Thus, these results show that at temperatures below 650°C the yield of hydrogen and syngas strongly determines by the contact time value:it is sufficiently high at the longer contact time.

Above 650°, the influence of the contact time on the catalyst performance has been studied at H_2O/EtOH molar ratio equals 6 when ethanol conversion is complete (Fig.9). The intermediate product – acetaldehyde is absent under these conditions, while selectivity to ethylene decreases at longer contact times and higher temperatures being close to zero at 800 °C for all contact

times. Hydrogen yield slightly varies with a contact time depending on the temperature. Thus, at 700 °C, hydrogen yield passes through a small maximum at the contact time 0.1 s, while at 750-800° it increases up to ~94-97% at the longest contact time (Fig. 9). Variation of CO selectivity with the contact time also depends on the temperature: at 700-750° it goes through the maximum at 0.1 s and decreases at 800°C with the rise of the contact time. Selectivity to CO_2 increases with the contact time rising at all temperatures. These variations observed for H_2, CO and CO_2 selectivities are due to parallel occurrence of water gas shift (WGS) and reverse WGS reactions whose shares in the overall ESR process depend not only on reaction thermodynamics [43-44] but kinetic factors as well [45-46]. A gradual rise of methane selectivity with the contact time at 700 °C is mainly controlled by methanation which is favoured over Ru-based catalysts in the presence of water [47]. At higher temperatures, steam reforming of methane leads to decrease of methane selectivity with longer contact times.

Temperature dependences of ethanol conversion, hydrogen yield and products selectivity at different H_2O/EtOH ratio and 0.07 s contact time over Ru/CZS-Al_2O_3 are presented in Figs. 10-11. At H_2O/EtOH=4-5 ethanol conversion (Fig. 10) passes through the minimum at 700-750 °C that is conditioned by formation of highly stable acetate groups on the CZS-Al_2O_3 surface which hinder the decomposition of ethoxide at the Ru/support interface. The increase of H_2O/EtOH ratio up to 6 leads to 100% ethanol conversion in the whole temperature range due to facile reforming of adsorbed intermediate carbonaceous species [40-42].

The values of hydrogen yield for H_2O/EtOH molar ratio =4-5 are close at 700-750 °C being somewhat higher when it is equal to 5. However, at increasing temperature above 750 °C, the hydrogen yield is noticeably higher for H_2O/EtOH=5. At H_2O/EtOH=6, the hydrogen yield is the highest in all temperature range, especially at 700-750 °C (Fig. 11). The same trends are observed for CO_2 selectivity while CO selectivity is practically independent on the H_2O/EtOH ratio (Fig. 11). At all water concentrations, selectivity to methane passes through the maximum at 750-800°C being lower at H_2O/EtOH=6 due to steam reforming which is more effective at high water concentrations and temperatures according to thermodynamics [43-44].

Selectivity to ethylene, which is formed via dehydration of ethanol over CZS-Al_2O_3 support, is practically independent on the water concentration being high at 650-700°C (~50-80%) and gradually decreases as the temperature increases dropping to zero at 800 °C. Such dependence is due to ethylene steam reforming which rate is high even at H_2O/EtOH=3 as was shown in [48]. Selectivity to acetaldehyde formed by dehydrogenation of ethanol is rather low not exceeding 7% and appreciably varies with values of H_2O/EtOH ratio. At H_2O/EtOH=4-5 it goes through the maximum at 700-750°C and falls to zero at 800°C being practically absent in the reaction

products at H_2O/EtOH=6 in the whole temperature range. Thus, dehydrogenation route of ESR could be competitive with dehydration reaction to ethylene depending on reaction parameters. The similar results were observed for NiZnAl and NiMgAl catalysts derived from layered double hydroxides: at H_2O/EtOH=3 and close contact time, the temperature dependence of selectivity to acetaldehyde passed through the maximum of 20% being equal to zero at high water concentration [49].

3.2.4. Testing of the monolithic catalyst.

The monolithic catalyst was tested in ESR without any pretreatment and was directly activated in the reaction mixture at the process temperature. The effect of water to ethanol ratio and contact time on the monolith performance was studied.

The effect of H_2O/EtOH ratio in the range from 1 to 6 on ESR over the monolithic catalyst was examined at the constant ethanol concentration at 720°C and the contact time of 0.4 s (Fig. 12). At all values of H_2O/EtOH ratio, the main products were H_2, CO, CO_2 and CH_4. The concentration of CO_2 and H_2 gradually increases with rising of the ratio H_2O/EtOH up to 6 while variation of CO concentration is opposite. In the whole, these dependences go with thermodynamic data (Fig. 12). However, if experimental CO_2 concentration is only slightly lower as compared to equilibrium one, the values of H_2 and CO concentration is appreciably below corresponding thermodynamic values (Fig. 12). The latter could be due to consumption of H_2 and CO in the methanation reaction [47]. The methane concentration higher than the equilibrium value confirms its occurring. In addition, the high methane concentration could be caused by ethanol cracking in the monolith channels.

The effect of contact time on the performance of the monolithic catalyst in ESR was studied at H_2O/EtOH=3 and exit temperature 750°C. The variation of the main products concentration with the contact time (Fig. 13), in general, corresponds to that for the grain catalyst Ru/CZS-Al_2O_3 (Fig. 9). H_2 and CO_2 concentration increases with longer contact time while concentrations of CO and CH_4 go down. As mentioned above, at 750°, if the change in concentrations of H_2, CO and CO_2 are mainly affected by water gas shift (WGS) and reverse WGS reactions, decreasing of CH_4 content in the exit reaction mixture is conditioned by its steam reforming.

The long-time testing of the monolithic catalyst was conducted at the temperature 750°, H_2O/EtOH=3, contact time of 0.4 s. The concentrations of H_2 and CO during 30 hours time-on-stream are practically unchanged (Fig. 14) evidencing high stability of the monolithic catalyst to coking.

4. Conclusions

Using original hydrothermal technology, honeycomb corundum monoliths with a peculiar porous structure were produced. Due to their high water-adsorbing capacity, a common method of incipient wetness impregnation was used for catalysts preparation instead of wash coating requiring repeated supporting of the prepared catalyst on the substrate that considerably simplifies procedures of catalyst loading on the monolith support:

The study of ethanol steam reforming reveals that the main route of the reaction over the catalyst Ru/CZ is dehydrogenation of ethanol with formation of acetaldehyde while ethanol dehydration into ethylene is mainly occurs over Ru/CZS-Al_2O_3. Variation of the H_2O/EtOH ratio, contact time and temperature allows hydrogen and CO yield to be governed. To obtain high yield of synthesis gas at short contact times the high temperatures are required.

The monolithic catalyst with 1%Ru - 8%$Ce_{0.4}Zr_{0.4}Sm_{0.2}O_2$ active component shows a high performance and stability at short contact time and rather low water concentration.

Acknowledgments: This work is supported by Integration Project 8 of SB RAS-NAN Belarus, Russian Fund of Basic Research Project RFBR-CNRS 12-03-93115

References.

1. A. Demirbas, *Progress in Energy and Combustion Science*, 33 (2007)1.
2. S. Sarkar, A. Kumar*, Bioresource Technology*, 101 (2010) 7350.
3. D. Bulushev, J. R. H. Ross, *Cat. Today*, 171 (2011) 1.
4. D. B. Levin, R. Chahine, *Int. J. Hydr. Energy*, 35 (2010) 4962.
5. S. A. Chattanathan, S. Adhikari, N. Abdoulmoumine, *Renew. Sustainable Energy Rev*., 16 (2012) 2366.
6. P. D. Vaidya, A. E. Rodrigues, *Chem. Eng. J.*, 117 (2006) 39.
7. K. K. Gupta, A. Rehman, R. M. Sarviy, *Renew. Sustainable Energy Rev.,* 14 (2010) 2946.
8. M. M. Yung, W. S. Jablonski, and K. A. Magrini-Bair, *Energy & Fuels*, 2009, 23, 1874.
9. A. Tanksale, J. N. Beltramini, GaoQing M. Lu, *Renew. Sustainable Energy Rev.*, 14 (2010) 166.
10. M. Slinn, K. Kendall, C. Mallon, J. Andrews, *Bioresource Technology,* 99 (2008) 5851.
11. A. Haryanto, S. Fernando, N. Murali, and S. Adhikari, *Energy & Fuels*, 19 (2005) 2098.
12. E. Kırtay, *Energy Conversion and Management,* 52 (2011) 1778.
13. A. C. Basagiannis, X. E. Verykios, *Appl. Catal A Gen.,* 308 (2006) 182.
14. X. Hu, G. Lu,. *Appl. Catal. B Environ.,* 88 (2009) 376.
15. K. Takanabe, K.Aika, K. Seshan, L.Lefferts, *J. Catal.* 227 (2004) 101.

16. P. Bichon, G. Haugom, H. J. Venvik, A. Holmen, E. A. Blekkan, *Top. Catal.,* 49 (2008) 38.
17. J. Comas, F. Marino, M. Laborde, N. Amadeo, *Chem. Eng. J*.**,** 98 (2004) 61.
18. A. N. Fatsikostas, X. E. Verykios, *J. Catal.,* 225 (2004) 439.
19. M. S. Batista, R. K. S. Santos, E. M. Assaf, J. M. Assaf, E. A. Ticianelli, *J. Power Sources***,** 134 (2004) 27.
20. S. Andonov, C. N. Bvil, K. Arishtirova, J. M. C. Bueno, S. Damyanova, *Appl. Catal. B: Envir*., 105 (2011) 346.
21. P. Biswas, D. Kunzru, *Chem. Eng. J*., 136 (2008) 41.
22. S. M. Lima, A. M. Silva, L. O.O. Costa , U. M. Graham, G. J. Burtron, H. Davis , L. V. Mattos, F. B. Noronha, *J. Catal*., 268 (2009) 268.
23. L. O. O. Costa, A. M. Silva, F. B. Noronha, L. V. Mattos, *Int. J. Hydr. Energy*, 37 (2012) 5930.
24. D. K. Liguras, D. I. Kondarides, X. E. Verykios, *Appl. Catal. B*, 43 (2003) 345.
25. C. Rioche, S. Kulkarni, F. C. Meunier , J. P. Breen, R. Burch, *Appl. Catal. B*, 61 (2005) 130.
26. S. M. Lima, A. M. Silva, L. O.O. Costa, U. M. Graham, G. J. Burtron, H. Davis, L. V. Mattos, F. B. Noronha, *Appl. Catal. A*, 352 (2009) 95.
27. C. P. Rodrigues, V. T. da Silva, M. Schmal, *Cat. Com*., 10 (2009) 1697.
28. I. A. C. Ramos, T. Montini, B. Lorenzut, H. Troiani, F. C. Gennari, M. Graziani, P. Fornasiero, *Cat. Today*, 180 (2012) 96.
29. M. E. Doukkali, A. Iriondo, P. L. Arias, J. F. Cambra, I. Gandarias, V. L. Barrio, *Int. J. Hydr. Energy*, 37 (2012) 8298.
30. J. Kašpar, P. Fornasiero, In *Catalysis by Ceria and Related Materials;* A.Trovarelli,; Ed.; Catalytic Science Series; Imperial College Press: London, UK, 2002. Vol. 2, pp 217.
31. T. Montini, L.D. Rogatis, V. Gombac, P. Fornasiero, M. Graziani, *Appl. Cat. B*, 71 (2007) 125.
32. D. K. Liguras, K. Goundani, X. E. Verykios, *J. Power Sources*, 130 (2004) 30.
33. D. K. Liguras, K. Goundani, X. E. Verykios, *Int. J. Hydr. Energy,* 29 (2004) 419.
34. A. Casanovas, C. Leitenburg, A. Trovarelli, J. Llorca, *Cat.Today*, 138 (2008) 187.
35. N. Goyal, K.K. Pant, R. Gupta, *Int. J. Hydr. Energy*, 38 (2013) 921.
36. M. E. Domine, E. E. Iojoiu, T. Davidian, N. Guilhaume, C. Mirodatos, *Cat. Today*, 133–135 (2008) 565.
37. P. Yaseneva, S. Pavlova, V. Sadykov, G. Alikina, A. Lukashevich, V. Rogov, S. Belochapkine, J. Ross, *Cat. Today*, 137 (2008) 23.
38. S.Rossignol, Y.Madier, D.Duprez, *Cat. Today,* 50 (1999) 261.

39. S. F. Tikhov, V. B. Fenelonov, V. I. Zaikovskii, Yu. V. Potapova, V. A. Sadykov, *Micropor. Mesopor. Mater.*, 33 (1999) 137.
40. S. Cavallaro, *Energy and Fuels*, 2000, 14, 1195.
41. M. Dömök, M. Tóth, J. Raskó, A. Erdőhelyi, *Appl. Cat. B*, 69 (2007) 262.
42. A. Erdohelyi, J. Raskor, T. Kecskers, M. Troth, M. Domok , K. Baarn, *Cat. Today*, 116 (2006) 367.
43. I. Fishtik, A. Alexander, R. Dattaa, D. Gean, *Int. J. Hydr. Energy*, 25 (2000) 31.
44. V. Mas, R. Kipreos, N.Amadeo, M. Laborde, *Int. J. Hydr. Energy*, 31 (2006) 21.
45. P. D. Vaidya and A. E. Rodrigues, *Ind. Eng. Chem. Res*., 45 (2006) 6614.
46. P.-J. Lu, T.-S. Chen, J.-M. Chern, *Cat. Today*, 174 (2011) 17.
47. V. Jimenez, P. Sanchez, P. Panagiotopoulou, J. L. Valverde, A. Romero, *Appl. Cat. A*, 390 (2010) 35.
48. J. P. Breen, R. Burch, H. M. Coleman, *Appl. Cat. B*, 39 (2002) 65.
49. C. Resini, T. Montanari, L. Barattini, G. Ramis, G. Busca, S. Presto, P. Riani, R. Marazza, M. Sisani, F. Marmottini, U. Costantino, *Appl. Cat. A,* 355 (2009) 83.

Figures captions.

Fig. 1 The monolith prepared by hydrothermal treatment (HTT) and extrusion after thermoshoks.

Fig. 2 SEM images of a monolith face plane near a channel (a) and an inner spall of monolith at different magnification (b, c).

Fig. 3 Raman spectrum of $Ce_{0.5}Zr_{0.5}O_2$ calcined at 900°C.

Fig. 4 Temperature dependence of ethanol conversion and hydrogen yield in the blank experiment and in the presence of CZS-Al_2O_3, Ru/ CZS-Al_2O_3, Ru/CZ. Reaction mixture EtOH:H_2O:N_2= 1:4:5, contact time 70 ms.

Fig. 5 Product selectivity in the blank experiment.

Fig. 6 Temperature dependence of the product selectivity in ESR for CZS-Al_2O_3, Ru/CZS-Al_2O_3 and Ru/CZ. Contact time 0.07 s, H_2O:EtOH=4.

Fig. 7 Temperature dependence of ethanol conversion (1, 2) and hydrogen yield (3, 4) at contact time of 0.46 (2, 4) and 1 s (1, 3). 10% vol. EtOH + 40% vol. H_2O, N_2 – balance.

Fig. 8 Influence of contact time on products selectivity: a – 0.46 s, b – 1 s. 10% vol. EtOH + 40% vol. H_2O, N_2 – balance.

Fig. 9 Influence of the contact time on the product selectivity in ESR. Catalyst - Ru/CZS-Al_2O_3. Contact time 0.07 - 0.2 s, reaction mixture 10% vol. EtOH + 60% vol. H_2O, N_2 – balance.

Fig. 10 Influence of the ratio H_2O/EtOH on the ethanol conversion. Ru/CZS-Al_2O_3, contact time 0.07 s, reaction mixture 10% vol. EtOH + 40-60% vol. H_2O, N_2 – balance.

Fig. 11 Influence of H_2O:EtOH ratio on the yield of hydrogen and selectivity of products in ESR. Catalyst - Ru/CZS-Al_2O_3. Contact time 0.07 s, Reaction mixture 10% vol. EtOH + 40-60% vol. H_2O, N_2 – balance.

Fig. 12 Products concentration vs. H_2O:EtOH ratio over the monolithic catalyst. 12% vol. EtOH, 720°C, contact time 0.4 s. Solid line – experimental data, dash line – thermodynamic data.

Fig. 13 Products concentration vs. contact time over the monolithic catalyst. 12% vol. EtOH + 36% H_2O, N_2 - balance, 750°C.

Fig. 14 H_2 and CO concentration vs. time-on-stream over the monolithic catalyst. EtOH concentration - 12 vol.%, H_2O:EtOH = 3, 750°C, contact time 0.4 s.

Table 1 H_2/CO ratio in ESR over Ru/CZS-Al_2O_3 and Ru/CZ catalysts at different contact times and H_2O:EtOH ratio.

Catalyst	Contact time, s	H_2O:EtOH	Temperature, °C				
			650	700	750	800	825
Ru/CZS-Al_2O_3	0.07	4	3,5	2,8	2,0	2,0	2,2
Ru/CZ	0.07	4	3,5	3,4	2,6	2,4	2,4
Ru/CZS-Al_2O_3	0.1	3	-	3	2	1,8	1,7
Ru/CZ	0.1	3	4.1	3.2	2,4	2.3	2.4

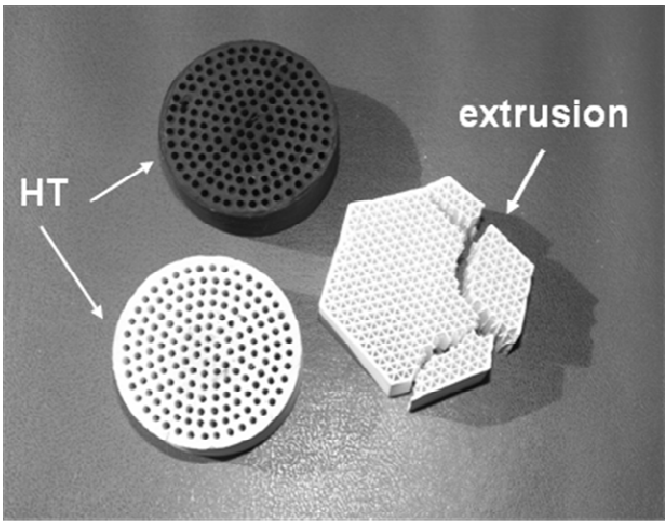

Fig. 1 The monolith prepared by hydrothermal treatment (HTT) and extrusion after thermoshoks.

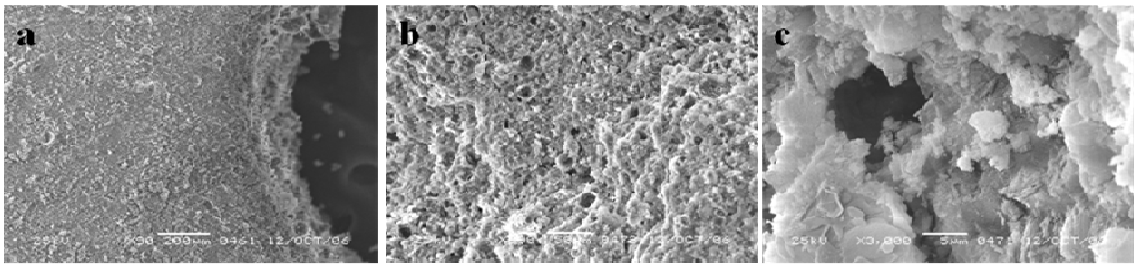

Fig.2 SEM images of a monolith face plane near a channel (a) and an inner spall of monolith at different magnification (b, c).

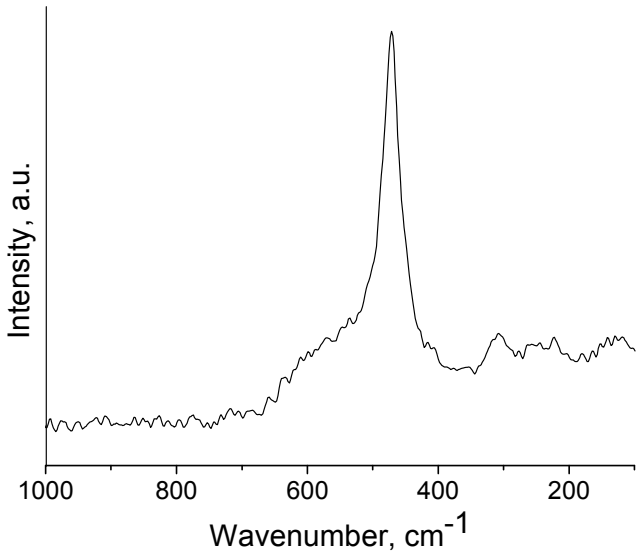

Fig. 3 Raman spectrum of $Ce_{0.5}Zr_{0.5}O_2$ calcined at 900°C.

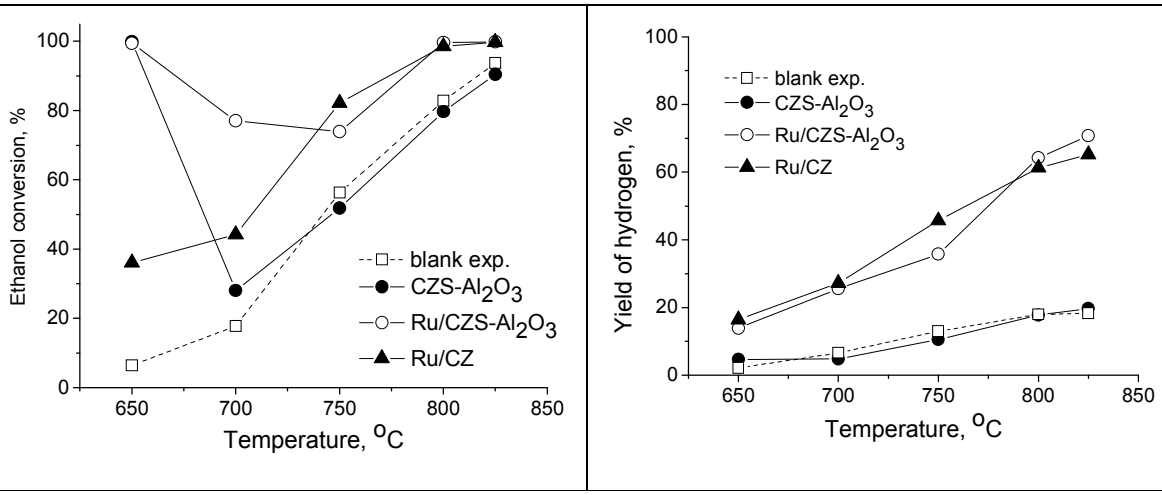

Fig. 4 Temperature dependence of ethanol conversion and hydrogen yield in the blank experiment and in the presence of $CZS\text{-}Al_2O_3$, Ru/ $CZS\text{-}Al_2O_3$, Ru/CZ. Reaction mixture $EtOH:H_2O:N_2$= 1:4:5, contact time 70 ms.

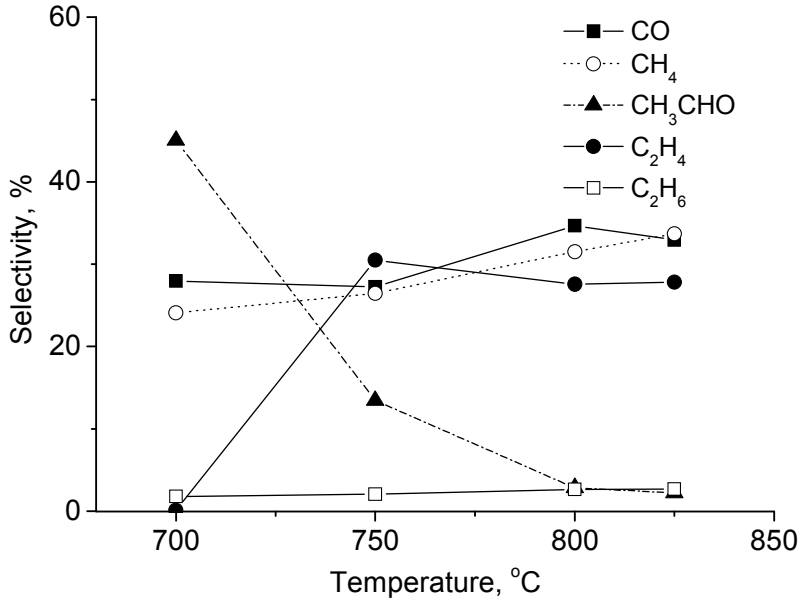

Fig. 5 Product selectivity in the blank experiment.

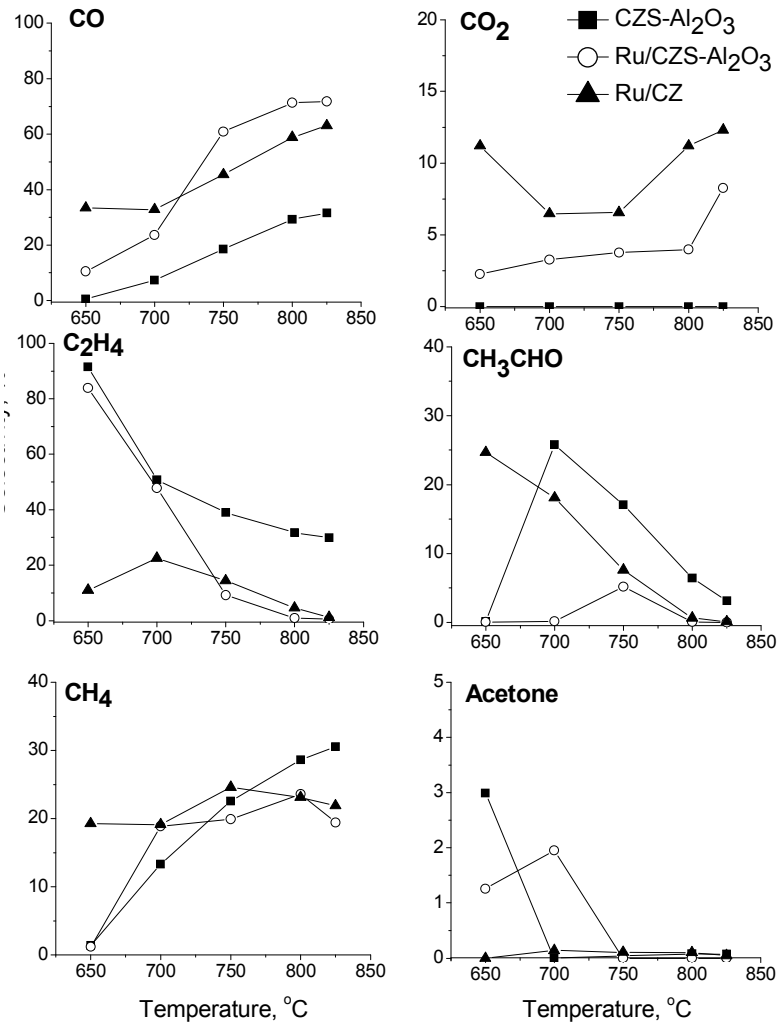

Fig. 6 Temperature dependence of the product selectivity in ESR for CZS-Al_2O_3, Ru/CZS-Al_2O_3 and Ru/CZ. Contact time 0.07 s, H_2O:EtOH=4.

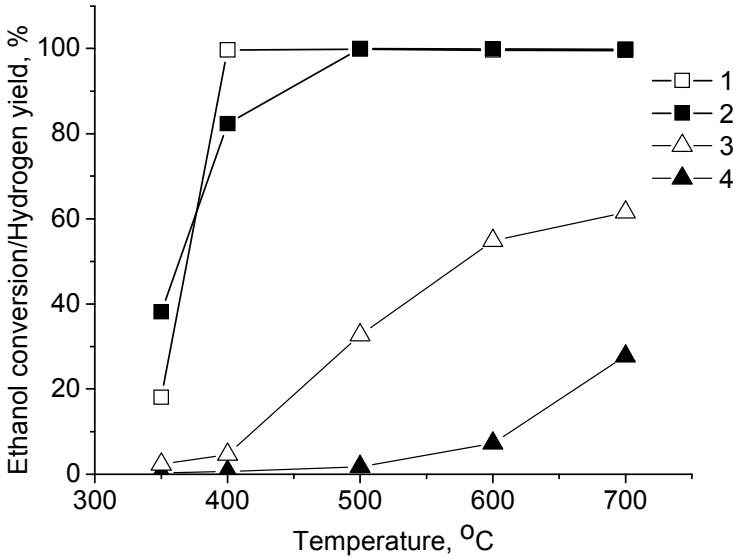

Fig. 7 Temperature dependence of ethanol conversion (1, 2) and hydrogen yield (3, 4) at contact time of 0.46 (2, 4) and 1 s (1, 3). 10% vol. EtOH + 40% vol. H_2O, N_2 – balance.

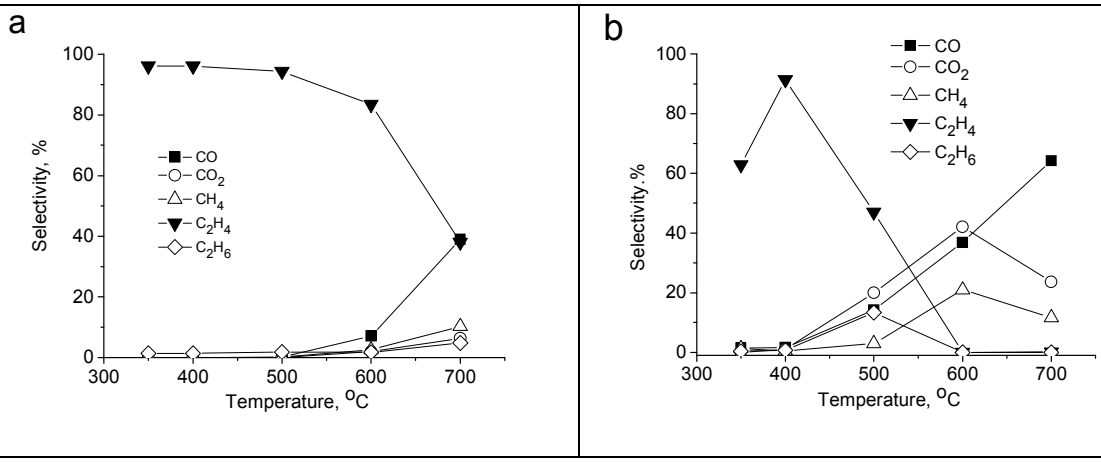

Fig. 8 Influence of contact time on products selectivity: a – 0.46 s, b – 1 s. 10% vol. EtOH + 40% vol. H_2O, N_2 – balance.

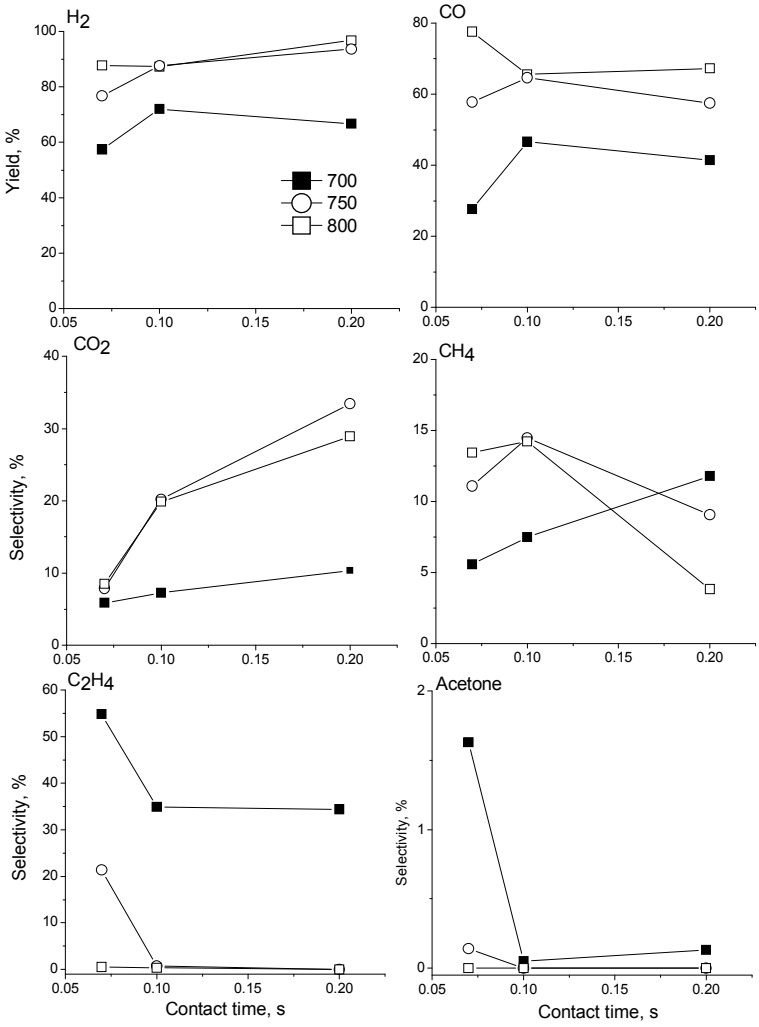

Fig. 9 Influence of the contact time on the product selectivity in ESR. Catalyst - Ru/CZS-Al_2O_3. Contact time 0.07 - 0.2 s, reaction mixture 10% vol. EtOH + 60% vol. H_2O, N_2 – balance.

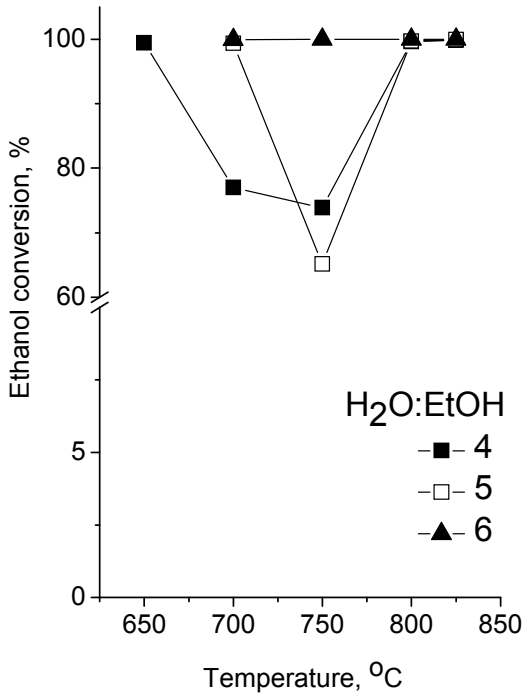

Fig. 10 Influence of the ratio H_2O/EtOH on the ethanol conversion. Ru/CZS-Al_2O_3, contact time 0.07 s, reaction mixture 10% vol. EtOH + 40-60% vol. H_2O, N_2 – balance.

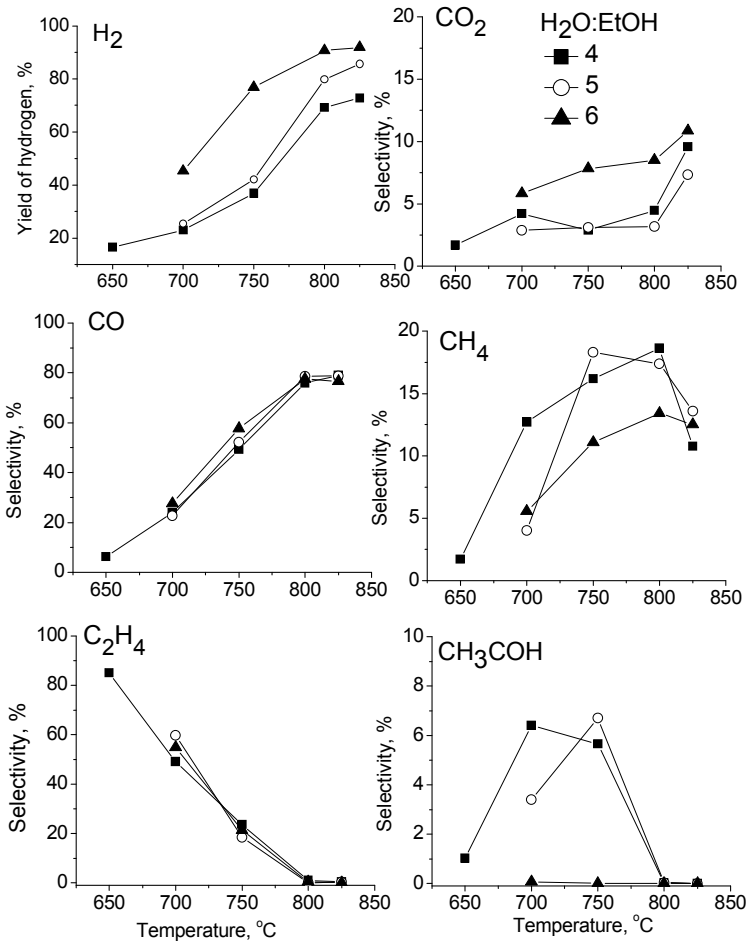

Fig. 11 Influence of H_2O:EtOH ratio on the yield of hydrogen and selectivity of products in ESR. Catalyst - Ru/CZS-Al_2O_3. Contact time 0.07 s, Reaction mixture 10% vol. EtOH + 40-60% vol. H_2O, N_2 – balance.

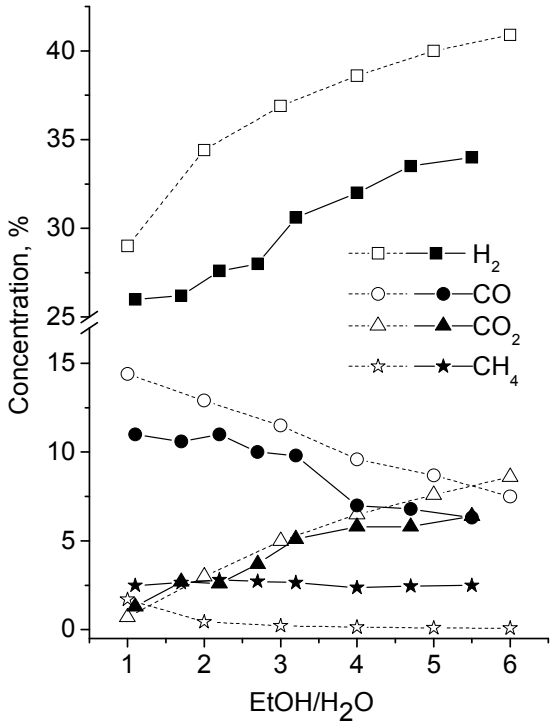

Fig. 12 Products concentration vs. H_2O:EtOH ratio over the monolithic catalyst. 12% vol. EtOH, 720°C, contact time 0.4 s. Solid line – experimental data, dash line – thermodynamic data.

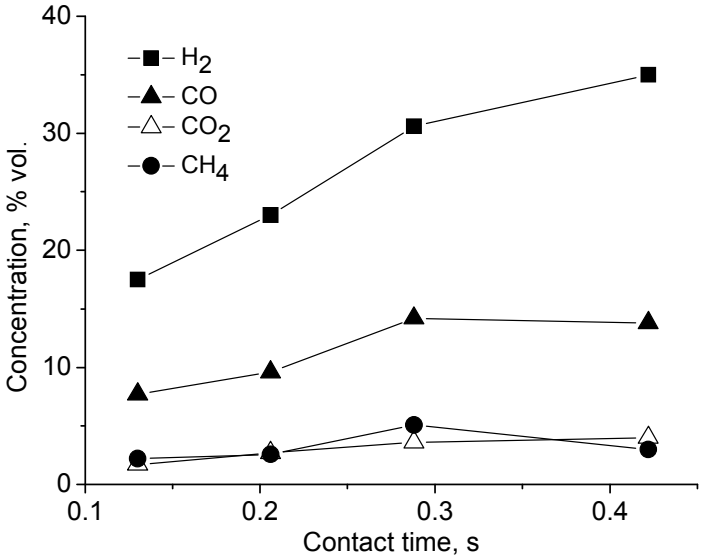

Fig. 13 Products concentration vs. contact time over the monolithic catalyst. 12% vol. EtOH + 36% H_2O, остальное – азот, 750°C.

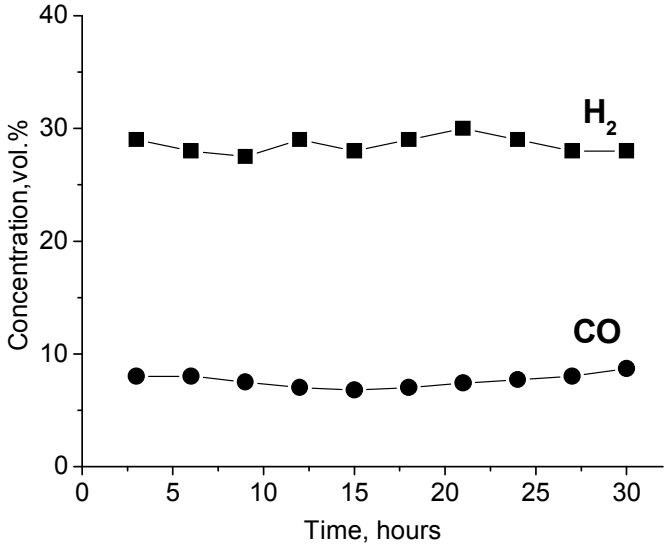

Fig. 14 H_2 and CO concentration vs. time-on-stream over the monolithic catalyst. EtOH concentration - 12 vol.%, H_2O:EtOH = 3, 750°C, contact time 0.4 s.